Journal of Traditional and Complementary Medicine 11 (2021) 158–172

Contents lists available at ScienceDirect

Journal of Traditional and Complementary Medicine

journal homepage: http://www.elsevier.com/locate/jtcme

Original Article

Mushroom-derived bioactive compounds potentially serve as the inhibitors of SARS-CoV-2 main protease: An *in silico* approach

Panthakarn Rangsinth [a, b], Chanin Sillapachaiyaporn [d], Sunita Nilkhet [d], Tewin Tencomnao [c], Alison T. Ung [e, **], Siriporn Chuchawankul [a, b, *]

[a] *Immunomodulation of Natural Products Research Group, Chulalongkorn University, Bangkok, 10330, Thailand*
[b] *Department of Transfusion Medicine and Clinical Microbiology, Faculty of Allied Health Sciences, Chulalongkorn University, Bangkok, 10330, Thailand*
[c] *Department of Clinical Chemistry, Faculty of Allied Health Sciences, Chulalongkorn University, Bangkok, 10330, Thailand*
[d] *Program in Clinical Biochemistry and Molecular Medicine, Department of Clinical Chemistry, Faculty of Allied Health Sciences, Chulalongkorn University, Bangkok, 10330, Thailand*
[e] *School of Mathematical and Physical Sciences, Faculty of Science, The University of Technology Sydney, Sydney, NSW, 2007, Australia*

ARTICLE INFO

Article history:
Received 18 August 2020
Received in revised form
29 December 2020
Accepted 30 December 2020
Available online 4 January 2021

Keywords:
COVID-19
Anti-HIV protease
Anti-SARS-CoV-2 main protease
Mushrooms
Molecular docking
ADMET analysis

ABSTRACT

Background and aim: Coronavirus Disease 2019 (COVID-19) caused by severe acute respiratory syndrome coronavirus 2 (SARS-CoV-2) has now become the world pandemic. There is a race to develop suitable drugs and vaccines for the disease. The anti-HIV protease drugs are currently repurposed for the potential treatment of COVID-19. The drugs were primarily screened against the SARS-CoV-2 main protease. With an urgent need for safe and effective drugs to treat the virus, we have explored natural products isolated from edible and medicinal mushrooms that have been reported to possess anti-HIV protease.
Experimental procedures: We have examined 36 compounds for their potential to be SARS-CoV-2 main protease inhibitors using molecular docking study. Moreover, drug-likeness properties including absorption, distribution, metabolism, excretion and toxicity were evaluated by *in silico* ADMET analysis.
Results: Our AutoDock study showed that 25 of 36 candidate compounds have the potential to inhibit the main viral protease based on their binding affinity against the enzyme's active site when compared to the standard drugs. Interestingly, ADMET analysis and toxicity prediction revealed that 6 out of 25 compounds are the best drug-like property candidates, including colossolactone VIII, colossolactone E, colossolactone G, ergosterol, heliantriol F and velutin.
Conclusion: Our study highlights the potential of existing mushroom-derived natural compounds for further investigation and possibly can be used to fight against SARS-CoV-2 infection.
Taxonomy (classification by evise): Disease, Infectious Disease, Respiratory System Disease, Covid-19, Traditional Medicine, Traditional Herbal Medicine, Phamaceutical Analysis.

1. Introduction

Severe acute respiratory syndrome coronavirus-2 (SARS-CoV-2), also known as 2019 novel coronavirus (2019-nCoV), has quickly spread worldwide since late 2019. Coronavirus Disease 2019 (COVID-19) has emerged as a severe global pandemic. As per the recent situational report released by the World Health Organization (WHO) on 27 December 2020, the disease has caused 1.7 million deaths and 78 million infections worldwide.[1] The disease's clinical characteristics can range from asymptomatic infections, mild respiratory disease, severe pneumonia with respiratory failure, and even fatal respiratory diseases such as acute respiratory distress

* Corresponding author. Immunomodulation of Natural Products Research Group, Department of Transfusion Medicine and Clinical Microbiology, Faculty of Allied Health Sciences, Chulalongkorn University, Bangkok, 10330, Thailand.
** Corresponding author. School of Mathematical and Physical Sciences, Faculty of Science, The University of Technology Sydney, Sydney, NSW, 2007, Australia.
E-mail addresses: Alison.Ung@uts.edu.au (A.T. Ung), Siriporn.Ch@chula.ac.th (S. Chuchawankul).
Peer review under responsibility of The Center for Food and Biomolecules, National Taiwan University.

https://doi.org/10.1016/j.jtcme.2020.12.002

List of abbreviations

SARS-CoV-2	Severe acute respiratory syndrome coronavirus-2
COVID-19	Coronavirus Disease 2019
HIV	Human immunodeficiency virus
ADME	Absorption Distribution Metabolism and Excretion
PDB	Protein Data Bank

syndrome.[2,3]

SARS-CoV-2 belongs to the family of the coronavirus. It is an enveloped virus with a positive-sense single-stranded RNA and a single linear RNA segment.[4] SARS-CoV-2 has been linked to two other strains, severe acute respiratory syndrome coronavirus (SARS-CoV) and Middle East respiratory syndrome coronavirus (MERS-CoV), in the zoonotic origins and the cause of fatal pneumonia.[4,5] The main viral protease has been proposed as a key therapeutic target for drug development against coronavirus and COVID-19 treatment.[6–11] The enzyme plays an essential role in the viral life cycle, mostly involving maturation cleavage events within several precursor proteins.[8,12] The active sites of this enzyme are highly conserved among all coronaviruses.[13] Furthermore, the main viral protease is a non-human homologue, making it an ideal antiviral target.[13]

Unfortunately, there is no anti-SARS-CoV-2 drug or vaccine sufficiently available to date. The urgent need for drugs to treat COVID-19 has led scientists to focus on protease inhibitors as potential drugs to cure the disease. Repurposing drugs currently used to treat HIV, HCV and SARS, taking advantage of drug safety, is one of the current anti-SARS-CoV-2 drug searching approaches. Repurposing HIV-drugs have been tested against SARS-CoV-2 main protease and shown effectiveness against the viral enzyme.[14,15] Moreover, the combination of anti-HIV protease drugs, lopinavir and ritonavir, was currently employed in a clinical trial against COVID-19 in patients with mild and moderate COVID-19. [16]

Lopinavir and Ritonavir, the approved drugs for HIV protease inhibitor, have been reported to inhibit the main protease of both SARS-CoV and MERS-CoV.[17–21] With the urgent need to reduce the impact of COVID-19, a combination of these drugs was currently investigated to treat SARS-CoV-2-infected patients.[20,22–25] However, these drugs' curative effect remains minimal, with potentially toxic side effects that might be harmful to the patients.[25] Identifying bioactive compounds from natural sources that can inhibit SARS-CoV-2 main protease is considered an alternative approach to combat COVID-19. [26–29] *In silico* technique, a computational approach, is the promising preliminary evidence for drug discovery.[30–34] Several molecular docking studies have identified bioactive compounds from natural products as the potential SARS-CoV-2 main protease inhibitors derived from natural sources.[35–40]

Mushrooms are a rich source of bioactive compounds with antiviral activity.[41,42] Some of the compounds showed anti-inflammatory activity.[43–45] These dual activities would be an effective treatment of COVID-19. A number of bioactive compounds have been shown to inhibit HIV protease, suggesting their potential activity against the main proteases of coronaviruses.[42] In this work, we carried out an *in silico* investigation of bioactive compounds found in edible and medicinal mushrooms. These compounds have been shown to display anti-HIV protease activity. We examined 36 compounds for their potential candidates as SARS-CoV-2 main protease inhibitors and investigated their drug-like properties using molecular docking study.

2. Materials and methods

2.1. Ligand preparation

A total of 36 mushroom-isolated compounds were selected from the literature, including those listed by Suwannarach et al.[42] (Table 1). Compounds No. 1–32 were reported for their anti-HIV protease property, whereas compound No. 33–36 showed anti-HIV activity via HIV reverse transcriptase inhibition. All chemical structures were obtained from the PubChem database. Prior to docking studies, each compound was loaded into Discovery Studio (DS) Visualizer (BIOVIA, CA, USA) and optimized using "Clean Geometry" function in DS. All compounds' files were converted to PDBQT format using AutoDockTools-1.5.6 software (The Scripps Research Institute, USA) for docking studies.

2.2. Protein preparation

The crystal structure of COVID-19 main protease in complex with an inhibitor N3 (PDB ID: 6LU7)[6] was obtained from RCSB Protein Data Bank. Before the docking studies, the protein structure was first prepared using the Prepare protein set up in AutoDock. The protein preparation is an optimization step that corrects structure, atomic and bond length and charges anomalies. Water molecules and the original inhibitor were removed from the protein structure. Then any missing hydrogen atoms were added. The optimization step was then employed to provide the stable conformation before converting to PDBQT format for docking analysis.

2.3. Molecular docking

Molecular docking studies were performed using the default protocol in Autodock tools 1.5.6 (AutoDock 4.2 software, The Scripps Research Institute, USA). The active site of SARS-CoV-2 main protease 6LU7 was set as a grid box. The grid box was set to 50 x 50 x 50 points in xyz-dimension that equated to a grid box spacing of 0.375 $Å^3$, and the coordinate of the x, y and z centers of the box are at −9.1, 11.0 and 68.0, respectively. The docking simulations were performed using the Lamarckian Genetic Algorithm with default parameters, including 10 Genetic Algorithm runs. The docking results of 10 runs were ranked by energy. The compound with the best energy ranking was further closely analyzed for its protein-ligand interactions using the DS Visualizer (BIOVIA, San Diego, CA, USA).

2.4. Drug-likeness prediction

The structures of compounds presented in mushrooms (Table 1) were obtained from PubChem database in SMILE files. The compounds were then evaluated for drug-likeness using the Lipinski's rule of five to predict their pharmacokinetic properties such as the Absorption, Distribution, Metabolism and Excretion (ADME) of the compounds using SwissADME (http://www.swissadme.ch/).[75]

2.5. Toxicity, carcinogenicity and mutagenicity prediction

The canonical SMILES of the list of compounds in Table 1 was further submitted to the pkCSM database and Toxtree software to predict their toxicity and carcinogenicity, respectively. The toxicity was predicted via toxicity mode in pkCSM database,[76] while carcinogenicity and mutagenicity prediction was analyzed using Toxtree 3.1.0 software based on the Benigni-Bossa rule.[77,78]

Table 1
List of anti- HIV bioactive compounds derived from mushrooms.

No.	Compound	Structure	Source	Reference
1	20(21)-dehydrolucidenic acid N	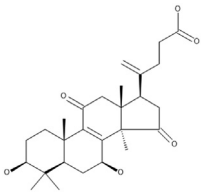	*Ganoderma sinense*	46
2	20-hydroxylucidenic acid N	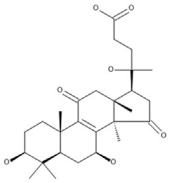	*Ganoderma sinense*	46
3	Agrocybin	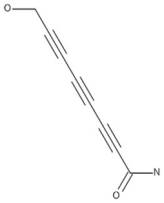	*Agrocybe cylindracea*	47
4	Betulinic acid	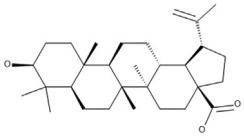	*Trametes versicolor*	48,49
5	Colossolactone A	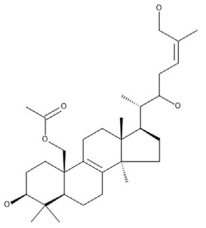	*Ganoderma colosum*	50
6	Colossolactone E	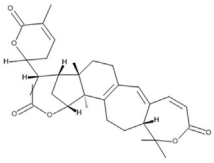	*Ganoderma colosum*	50
7	Colossolactone G	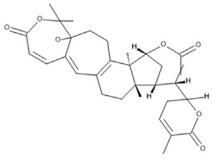	*Ganoderma colosum*	50
8	Colossolactone V	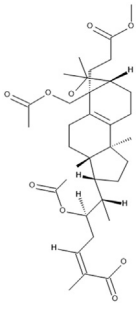	*Ganoderma colosum*	50

Table 1 (*continued*)

No.	Compound	Structure	Source	Reference
9	Colossolactone VII	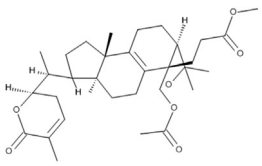	*Ganoderma colosum*	50
10	Colossolactone VIII	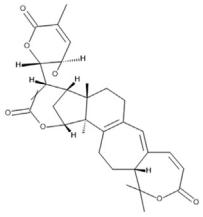	*Ganoderma colosum*	50
11	Ellagic acid	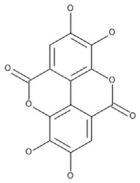	*Flammulina velutipes*, *Phellinus linteus*, *Pleurotus eryngii*	51–54
12	Ergosterol	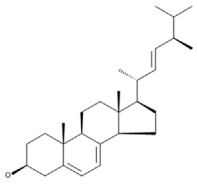	*Auricularia polytricha*, *Flammulina velutipes*, *Lentinula edodes*	55–57
13	Gallic acid	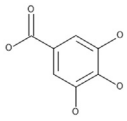	*Agaricus bisporus*, *Flammulina velutipes*, *Ganoderma lucidum*, *Laetiporus sulphureus*, *Lentinus lepideus*, *Leucoagaricus leucothites*, *Macrocybe gigantea*, *Pleurotus ostreatus*	51,58–62
14	Ganoderic acid alpha	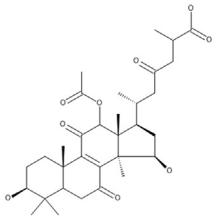	*Ganoderma lucidum*	63
15	Ganoderic acid B	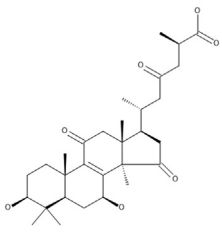	*Ganoderma lucidum*	63,64
16	Ganoderic acid beta	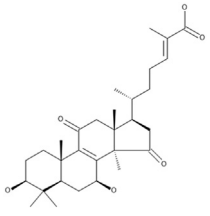	*Ganoderma lucidum*	65

(*continued on next page*)

Table 1 (*continued*)

No.	Compound	Structure	Source	Reference
17	Ganoderic acid C1	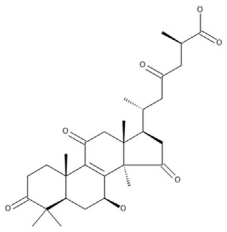	*Ganoderma lucidum*	63
18	Ganoderic acid GS-2	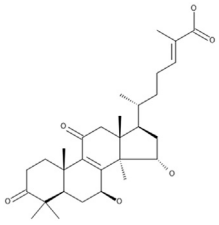	*Ganoderma sinense*	46
19	Ganoderic acid H	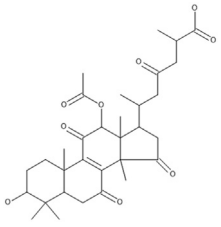	*Ganoderma lucidum*	63
20	Ganoderiol A	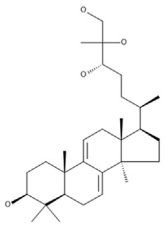	*Ganoderma lucidum*	63
21	Ganoderiol B	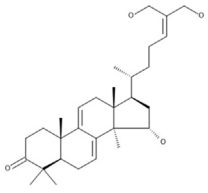	*Ganoderma lucidum*	63
22	Ganoderiol F	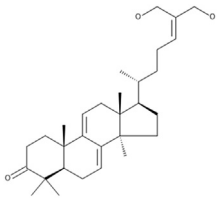	*Ganoderma lucidum, Ganoderma sinense*	46,63
23	Ganodermanondiol	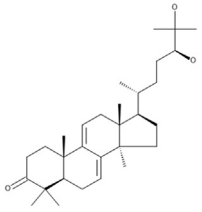	*Ganoderma lucidum*	65

Table 1 (*continued*)

No.	Compound	Structure	Source	Reference
24	Ganodermanontriol	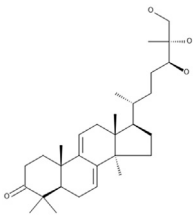	*Ganoderma lucidum*	63,65
25	Ganolucidic acid A	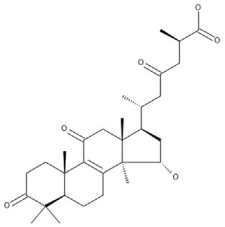	*Ganoderma lucidum*	65
26	Ganomycin B	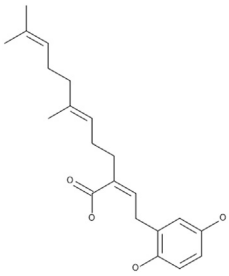	*Ganoderma colosum*	50,66
27	Ganomycin I	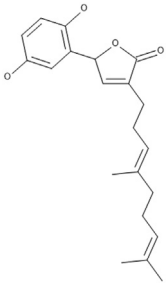	*Ganoderma colosum*	50,66
28	Heliantriol F	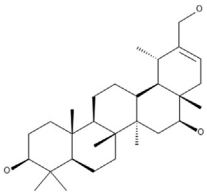	*Lignosus rhinocerus*	67
29	Linoleic acid	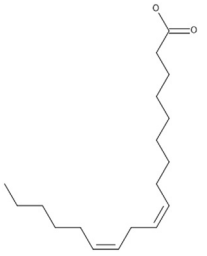	*Auricularia polytricha*, *Lentinula edodes*	55,57

(*continued on next page*)

Table 1 (*continued*)

No.	Compound	Structure	Source	Reference
30	Lucidumol B	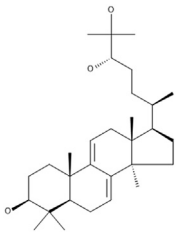	*Ganoderma lucidum*	65
31	Methyl gallate	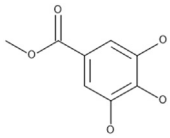	*Pholiota adiposa*	68
32	Oleanolic acid	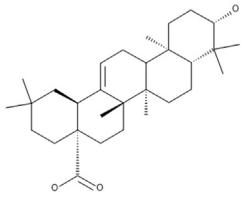	*Hericium erinaceus,* *Lactarius deliciosus,* *Lactarius sanguifluus,* *Lactarius semisanguifluus* *Russula delica, Suillus bellinii*	69–71
33	Semicochliodinol A	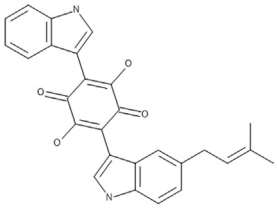	*Chrysosporium merdarium*	72
34	Semicochliodinol B	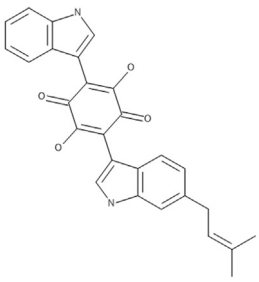	*Chrysosporium merdarium*	72
35	Ursolic acid	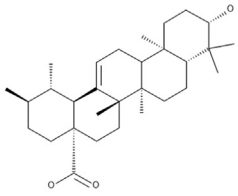	*Cynomorium songaricum,* *Hericium erinaceus,* *Russula delica, Suillus bellinii*	70,71,73
36	Velutin	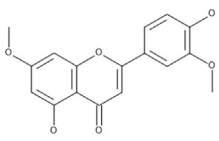	*Flammulina velutipes*	74

3. Results and discussion

3.1. Investigation of mushroom-derived bioactive compounds against SARS-CoV-2 main protease by molecular docking

The crystal structure of COVID-19 main protease in complex with the inhibitor N3 (PDB ID: 6LU7 obtained on 21 June 2020) [6] was obtained from RCSB Protein Data Bank. The protein structure was prepared for the docking studies by removing water molecules and the inhibitor before optimization step to provide the stable conformation. The docking protocol was validated using the standard set up in AutoDock. The minimized structure of the inhibitor N3 was re-docked into the original binding site of the protein. The results of 10 Genetic Algorithm runs of the re-docking were ranked

Table 2
Hydrogen bond interaction between N3 and 6LU7.

6LU7-N3 interaction	Binding energy (kcal/mol)	Hydrogen bonding		3D diagrams
		Number	Amino acid interaction	
X-ray structure	–	10	GLY143, THR190, GLN189, PHE140, HIS163, HIS164, MET165, HIS172, GLU166 (2)	
Re-docked structure 1	−7.97	3	GLY143, LEU141, GLU166	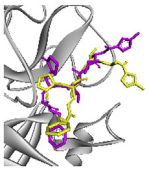
Re-docked structure 2	−6.28	2	GLN189, THR190	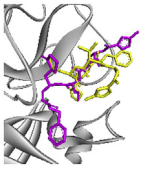
Re-docked structure 3	−5.89	5	ASN142, HIS163, GLU166, GLY143, CYS145	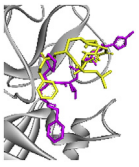
Re-docked structure 4	−5.86	2	CYS145, THR190	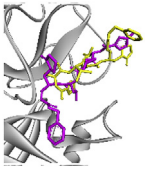
Re-docked structure 5	−5.85	2	GLU166, GLN189	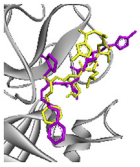
Re-docked structure 6	−5.65	5	HIS41, CYS145, GLU166, GLN189, MET165	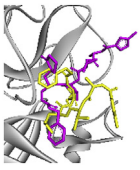
Re-docked structure 7	−5.03	3	GLN189, PRO168, GLY143	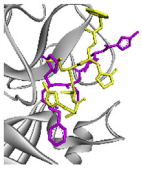
Re-docked structure 8	−4.36	6	ASN142, CYS145, HIS163, SER46, MET165, HIS172	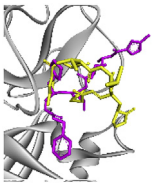
Re-docked structure 9	−4.30	4	GLU166, PRO168, GLU166(2)	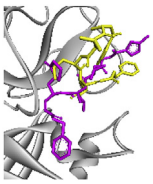

(*continued on next page*)

Table 2 (*continued*)

6LU7-N3 interaction	Binding energy (kcal/mol)	Hydrogen bonding		3D diagrams
		Number	Amino acid interaction	
Re-docked structure 10	−3.55	3	ASN142, GLU166(2)	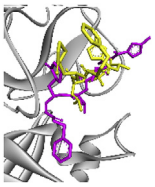

The 10 Genetic Algorithm runs on the re-docking of 6LU7-N3 using the validated method were shown. The results were ranked by binding energy. The lowest binding energy showed the best overlapping between N3 ligand from crystal (violet) and re-docking via AutoDock (yellow).

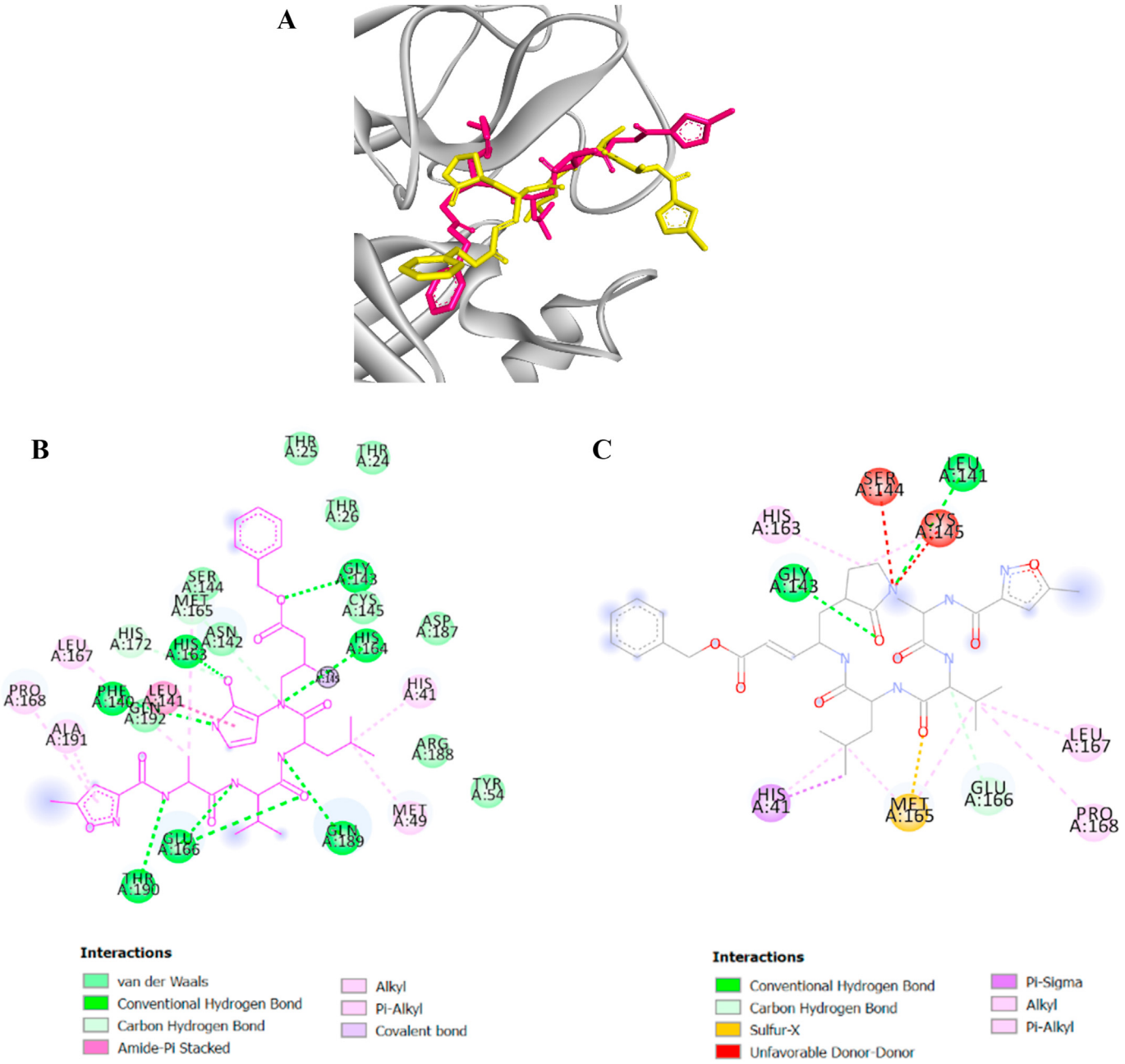

Fig. 1. The results from validation method for molecular docking study of SARS-CoV-2 main protease (6LU7). (A) The 3D diagrams of interaction between N3 and 6LU7 at the active site demonstrated overlapping between N3 ligand from crystal (magenta) and re-docking via AutoDock (yellow). (B) and (C) displayed the 2D ligands-receptor interactions of N3 from crystal and re-docking ligand via AutoDock structure with 6LU7, respectively.

Table 3
Docking results of all mushroom-derived compounds with the SARS-CoV-2 main protease.

No	Compound	Binding energy (kcal/mol)	Ligand Efficiency	Inhibition constant (Kpi)
	N3 (original inhibitor)	−7.97	−0.16	1.44 μM
	Lopinavir	−7.41	−0.16	3.32 μM
	Ritonavir	−6.19	−0.12	28.94 μM
	Andrographolide	−7.93	−0.32	1.55 μM
	Kaempferol	−7.99	−0.38	1.38 μM
1	Colossolactone VIII	−10.55	−0.27	18.58 nM
2	Colossolactone E	−10.10	−0.27	39.58 nM
3	Colossolactone G	−9.86	−0.25	58.86 nM
4	Ergosterol	−9.49	−0.33	111.07 nM
5	Semicochliodinol A	−8.91	−0.27	294.8 nM
6	Heliantriol F	−8.91	−0.27	292.54 nM
7	Semicochliodinol B	−8.71	−0.26	412.95 nM
8	Ganoderic acid GS-2	−8.68	−0.24	433.02 nM
9	Lucidumol B	−8.64	−0.26	464.56 nM
10	Ganodermanondiol	−8.60	−0.26	500.55 nM
11	Ursolic acid	−8.50	−0.26	598.68 nM
12	Colossolactone A	−8.49	−0.23	594.72 nM
13	Oleanolic acid	−8.35	−0.25	756.26 nM
14	Ganodermanontriol	−8.30	−0.24	818.74 nM
15	Ganolucidic acid A	−8.27	−0.23	865.36 nM
16	Ganoderic acid beta	−8.17	−0.23	1.02 μM
17	Ganoderic acid B	−7.99	−0.22	1.39 μM
18	Velutin	−7.97	−0.35	1.45 μM
19	Ganoderiol F	−7.95	−0.24	1.48 μM
20	20(21)-dehydrolucidenic acid N	−7.88	−0.24	1.67 μM
21	Ganoderic acid C1	−7.88	−0.21	1.66 μM
22	Ganoderiol A	−7.87	−0.23	1.72 μM
23	Ganoderiol B	−7.68	−0.23	2.34 μM
24	Ganoderic acid H	−7.65	−0.19	2.48 μM
25	Betulinic acid	−7.62	−0.23	2.61 μM
26	Ganomycin I	−7.37	−0.29	3.96 μM
27	Colossolactone VII	−7.33	−0.18	4.24 μM
28	20-hydroxylucidenic acid N	−6.98	−0.21	7.71 μM
29	Ganoderic acid alpha	−6.79	−0.17	10.55 μM
30	Ellagic acid	−6.76	−0.31	11.04 μM
31	Ganomycin B	−6.02	−0.24	38.57 μM
32	Linoleic acid	−5.37	−0.27	116.76 μM
33	Colossolactone V	−4.86	−0.11	274.96 μM
34	Agrocybin	−4.81	−0.44	300.41 μM
35	Methyl gallate	−4.79	−0.37	308.49 μM
36	Gallic acid	−4.26	−0.36	757.15 μM

and shown in Table 2. The best docking score of N3 was re-docked structure 1 which showed binding energy at −7.97 kcal/mol. The conformation, orientation, position and interactions of the redocked N3 at the binding site were analyzed and compared to that found in the original X-ray structure (PDB ID: 6LU7). Superimposing of the redocked protein-N3 over the original X-ray structure indicated that N3 was able to seek out the location of the receptor site. It is noteworthy that the re-docked N3 has adopted a slightly different conformation, specifically at the 5-methylisoxazole-3-carboxamide part of the molecule compared to that found in the X-ray structure, as shown in Fig. 1B. The variation in conformation, perhaps due to the stable conformation of N3 adopted *in silico*.The best re-docked N3 was found to interact with only two active site amino acid residues (GLY143 and GLU166) out of nine different residues observed in the X-ray structures. The common key interactions are shown in Table 2. This indicates that N3 was able to recognize its original receptor site in the X-ray structure of 6LU7, using this docking protocol. The results above validated the docking protocol as a suitable method for this study.

The validated docking protocol was subsequently used for *in silico* screening of potential compounds as inhibitors against SARS-CoV-2 main protease. The *in silico* inhibition of SARS-CoV-2 main protease is gauged on the potential binding affinity of the compounds. The binding energy expressed the binding affinity as Gibbs free energy by which the compounds displayed the higher negative binding energy were considered betters.[79] The *in silico* binding affinities of Lopinavir and Ritonavir to 6LU7 were determined. Since Lopinavir and Ritonavir are anti-HIV protease drugs that have been currently used in hospitals for COVID-19 treatment.[22–25] Therefore, it is appropriate to use them as standard drugs in addition to N3 for comparative study. Lopinavir and Ritonavir showed binding energy at −7.41 and −6.19 kcal/mol against 6LU7, respectively. Andrographolide and kaempferol have been previously demonstrated the potential inhibition against 6LU7 via docking studies.[36,80] They were also docked in this study to confirm our validated method. Our docking results agreed with recent reports that both andrographolide and kaempferol had lower binding energy (−7.93 and −7.99 kcal/mol, respectively) than that of anti-HIV agents, indicating their potency to inhibit SARS-CoV-2 main protease.

The docking scores of all compounds are presented in Table 3. Out of 36 compounds, seventeen compounds (No.1–17) showed lower binding energy (<−7.97 kcal/mol) binding to 6LU7 than that of original inhibitor (N3), Lopinavir and Ritonavir. Notably, 25 out of 36 mushroom-derived compounds (No.1–25) showed lower binding energy against 6LU7 than that of lopinavir, while 30 out of 36 compounds (No.1–30) showed lower binding energy than that of Ritonavir. From these results, colossolactone VIII exhibited the lowest binding energy against SARS-CoV-2 protease (−10.55 kcal/

Table 4
The physiochemical properties of the top 25 potential compounds derived from mushrooms as SARS-CoV-2 main protease inhibitors based on Lipinski's rule of five.

No	Compound	MW (g/mol) (≤ 500 g/mol)	Num. H-bond acceptors (≤ 10)	Num. H-bond donors (≤ 5)	Log $P_{o/w}$ (≤ 5)	Violation (≤ 1)
1	Colossolactone VIII[a]	558.75	7	1	5.49	2
2	Colossolactone E[a]	522.67	4	0	5.27	2
3	Colossolactone G	538.67	7	1	4.57	1
4	Ergosterol	396.65	1	1	6.49	1
5	Heliantriol F	458.72	3	3	5.28	1
6	Semicochliodinol A	438.47	4	4	4.15	0
7	Semicochliodinol B	438.47	4	4	4.13	0
8	Ganoderic acid GS-2	500.67	6	3	4.07	1
9	Lucidumol B	458.72	3	3	5.63	1
10	Ganodermanondiol	456.70	5	2	5.71	1
11	Ursolic acid	456.70	3	2	5.94	1
12	Colossolactone A[a]	516.75	5	3	5.46	2
13	Oleanolic acid	456.70	3	2	6.06	1
14	Ganodermanontriol	472.70	4	3	4.90	0
15	Ganolucidic acid A	500.67	6	2	4.10	1
16	Ganoderic acid beta	500.67	6	3	4.02	1
17	Ganoderic acid B	516.67	7	3	3.34	1
18	Velutin	314.29	6	2	2.60	0
19	Ganoderiol F	454.68	3	2	5.63	1
20	Ganoderic acid C1	514.65	7	2	3.27	1
21	20(21)-dehydrolucidenic acid N	476.60	7	4	2.41	0
22	Ganoderiol A	474.72	4	4	4.89	0
23	Ganoderiol B	470.68	4	3	4.90	0
24	Ganoderic acid H	572.69	9	2	3.20	1
25	Betulinic acid	456.70	3	2	6.11	1

Note.
[a] Non-drug-likeness compounds based on Lipinski's rule of five.

mol) followed by colossolactone E, colossolactone G, ergosterol, semicochliodinol A and heliantriol F (−10.10, −9.86, −9.49, −8.91 and −8.91 kcal/mol, respectively). Consistent with previous reports,[81–83] our results from molecular docking found that ursolic acid, oleanolic acid and betulinic acid also exhibited the potential to inhibit SARS-CoV-2 main protease.

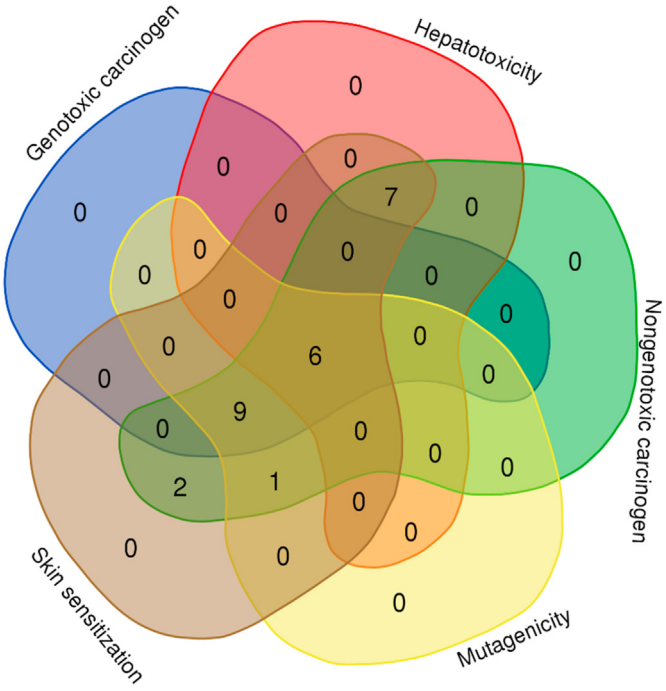

Fig. 2. Venn diagram describes the number of compounds predicted no toxicity, no carcinogenicity and no mutagenicity. There are six compounds predicted non-toxicity to skin and liver as well as non-mutagenicity and non-carcinogenicity.

3.2. ADME analysis

The ADME (Adsorption, Distribution, Metabolism and Excretion) analysis was performed to evaluate the drug-likeness of 36 compounds found in mushrooms. The prediction was performed using SwissADME database. Drug-likeness was indicated by Lipinski's rule of five. With respect to the criteria, molecular weight (MW) ≤ 500, the number of hydrogen bond acceptor ≤ 10, the number of hydrogen bond donors ≤ 5 and the Log $P_{o/w}$ ≤ 5 [84], no more than 1 violation is allowed. We found compounds listed 1–25 with lower binding energy than those of both drug standards as ranked in Table 4. The drug-like property's prediction was then evaluated.

ADME is an essential tool for analyzing the proposed molecule's oral bioavailability as possible drugs. As shown in Table 4, the prediction results showed that compounds list 1–22 passed the Lipinski's rule of five. The best five compounds based on docking score and Lipinski's rule of five for SARS-CoV-2 main protease inhibition are colossolactone G, ergosterol, heliantriol F, semicochliodinol A and semicochliodinol B. Although three compounds, i.e. colossolactone VIII, colossolactone E and colossolactone A, violated more than one rule, there is an exception to Lipinski's rule for natural products. Therefore, these three are acceptable as druglikness compounds.

3.3. Toxicity, carcinogenicity and mutagenicity prediction

The toxicity of the potential compounds was predicted via toxicity mode in pkCSM database.[76] The toxicity prediction was described in Supplementary data 1. The top 25 compounds' carcinogenicity and mutagenicity were determined using Toxtree 3.1.0 software based on the Benigni-Bossa rule. The rule determines the compound's carcinogenic and mutagenic potency based on the compound's functional groups. The functional groups confer as either carcinogenic or mutagenic are acyl halide, haloalkene, epoxide, aliphatic halogen, alkyl nitrate, aldehyde, hydrazine, isocyanate, polyaromatic hydrocarbon, azide, alkyl/aromatic nitro,

Table 6
H-bond interactions of top 25 potential compounds derived from mushrooms against SARS-CoV-2 main protease inhibitor.

No	Compound	Hydrogen bonding	
		Number	Amino acid interaction: bond length
	X-ray structure (N3)	10	GLY143: 2.86529, THR190:2.84976 , GLN189: 2.88951, PHE140: 3.18679, HIS163: 2.36734, HIS164: 2.80304, MET165: 3.69210, HIS172: 3.72440, GLU166: 2.97927, GLU166: 2.83433
1	Colossolactone VIII	2	HIS41: 2.72763, GLN189: 1.96169
2	Colossolactone E	1	HIS41: 3.02314
3	Colossolactone G	4	HIS41: 2.58995, ASN142: 1.88729, GLN189: 1.65515, HIS172: 2.84417
4	Ergosterol	1	ASP187: 2.18813
5	Heliantriol F	2	THR190: 1.85702, GLN189: 2.18737
6	Semicochliodinol A	6	SER144: 1.82069, MET165: 3.03681, GLY143: 2.7737, CYS145: 3.69761, GLU166: 2.01863, GLU166: 3.36082
7	Semicochliodinol B	3	ARG188: 1.86701, CYS145: 3.18962, CYS145: 3.89699
8	Ganoderic acid GS-2	4	HIS41: 2.83185, GLU166: 2.24025, GLN189: 2.41463, ASN142: 2.11084
9	Lucidumol B	3	GLN189: 1.96259, GLN189: 2.14332, GLU166: 2.83998
10	Ganodermanondiol	8	GLY143: 2.49923, CYS145: 2.76771, HIS163: 2.08786, SER144: 1.90278, LEU141: 1.64009, SER144: 2.43463, LEU167: 3.51115, PRO168: 2.91688
11	Ursolic acid	3	SER144: 2.87305, CYS145: 2.02309, CYS145: 2.97091
12	Colossolactone A	3	HIS163: 1.91024, CYS145: 2.52781, THR190: 1.85473
13	Oleanolic acid	3	SER144: 2.97806, CYS145: 1.97439, CYS145: 2.65435
14	Ganodermanontriol	8	GLY143: 2.6619, HIS163: 2.25078, LEU141: 2.11468, SER144: 2.86257, LEU141: 1.79129, ASN142: 2.96571, LEU167: 3.47167, PRO168: 2.72296
15	Ganolucidic acid A	3	GLU166: 2.24559, GLN189: 2.44479, ASN142: 1.94471
16	Ganoderic acid beta	4	TYR54: 2.24534, GLU166: 2.24309, MET49: 2.05161, ARG188: 2.99000
17	Ganoderic acid B	6	HIS41: 2.52071, GLY143: 2.65843, CYS145: 3.63501, GLU166: 2.42919, MET49: 2.0714, ASN142: 1.77428
18	Velutin	2	THR190: 2.15553, MET49: 3.56078
19	Ganoderiol F	1	ASP187: 1.81627
20	Ganoderic acid C1	4	TYR54: 2.29094, GLN189: 2.96608, ASN142: 2.04706, ARG188: 3.33477
21	20(21)-dehydrolucidenic acid N	5	GLY143: 2.52618, GLU166: 2.2808, CYS145: 2.70312, MET49: 2.20979, ASN142: 1.81534
22	Ganoderiol A	4	MET49: 2.2339, GLU166: 1.94189, GLU166: 1.89131, GLU166: 3.10886
23	Ganoderiol B	6	CYS145: 2.73888, CYS145: 3.60588, MET165: 2.75963, LEU141: 2.23062, LEU141: 2.48645, SER144: 2.06885
24	Ganoderic acid H	5	ASN142: 1.83347, ASN142: 2.34095, GLU166: 2.10428, GLU166: 2.68895, THR190: 1.78362
25	Betulinic acid	2	PRO168: 2.29376, GLN189: 1.67449

coumarin, diazo aromatic, benzyl sulfinyl ether, alkyl halide and thiocarbonyl.[77,78,85] Predicted genotoxic carcinogenicity, non-genotoxic carcinogenicity and mutagenic potential of the compounds were shown in Supplementary data 2. Overall, six compounds are shown in Fig. 2, including colossolactone VIII, colossolactone E, colossolactone G, ergosterol, heliantriol F and velutin were predicted as non-toxic, non-carcinogenic and non-mutagenic compounds derived from mushrooms.

3.4. Hydrogen bond analysis

The complex interactions between the SARS-CoV-2 protease and compounds listed 1–25 were visualized, and hydrogen bond analysis was conducted using Discovery Studio Visualizer. The number of hydrogen bonds and the residues involved in hydrogen bond interactions are summarized in Table 6. Colossolactone G, ergosterol, heliantriol F and velutin are the potential candidate compounds for SARS-CoV-2 inhibitors with drug-likeness property, no toxicity, no carcinogenicity and no mutagenicity. Colossolactone G has four hydrogen bonds interacting with the active site of SARS-CoV-2 main protease at the residue HIS41, ASN142, GLN189 and HIS172 (Fig. 3A). Ergosterol shows a hydrogen bond binding to viral protease at the residue ASP187 (Fig. 3B). Hydrogen bond interaction of heliantriol F against the main protease are two interactions at the residue THR190 and GLN189, while velutin exhibited two interactions at the residue THR190 and MET49 (Fig. 3D-E). It is noteworthy that colossolactone G, heliantriol F and velutin exhibited the common interactions when compared to X-ray structure of 6LU7-N3. The common interaction of colossolactone G and velutin is GLN189 residue, while heliantriol F is THR190 residue. Even though colossolactone VIII and colossolactone E were predicted as non-druglikness compounds; it was acceptable to include them as the potential anti-SARS-CoV-2 main protease candidates as we previously mentioned. Colossolactone VIII has two hydrogen bonds interacting with the viral protease's active site at the residue HIS41 and GLN189, while colossolactone E has a hydrogen bond interaction at the residue HIS41 (Fig. 3E-F). Semicochliodinol A was predicted as a hepatotoxicity agent; it has shown the significant six interactions at the receptor site. Those involved residues are SER144, MET165, GLY143, CYS145, GLU166 and GLU166 (Fig. 3G), in which MET165, GLY143 and GLU166 are the common interactions when compared to X-ray structure of 6LU7-N3. Compared to the original inhibitor, the studied compounds' common interactions could demonstrate mushroom-derived compounds as the potential inhibitors against SARS-CoV-2 main protease.

Our project plan's next step is to confirm the anti- SARS-CoV-2 of the identified compounds using SARS-CoV-2 assay kit (BPS Bioscience, CA, USA). The compounds that show inhibitory activity will be screened for their toxicity against normal human cell models such as human peripheral blood mononuclear cells (PBMCs).

4. Conclusions

The current therapeutic drugs against COVID-19 is a group of anti-HIV protease drugs. However, the compound with more efficiency and less toxicity is needed. Moreover, the most severe cases of COVID-19 are caused by infection-induced hyper-inflammation of the lungs and followed by acute respiratory distress, resulting in death. Therefore, effective treatment of COVID-19 would likely be a combination of therapies, using both antiviral and anti-inflammatory drugs. Several bioactive compounds derived from mushrooms have been promisingly demonstrated to exhibit anti-

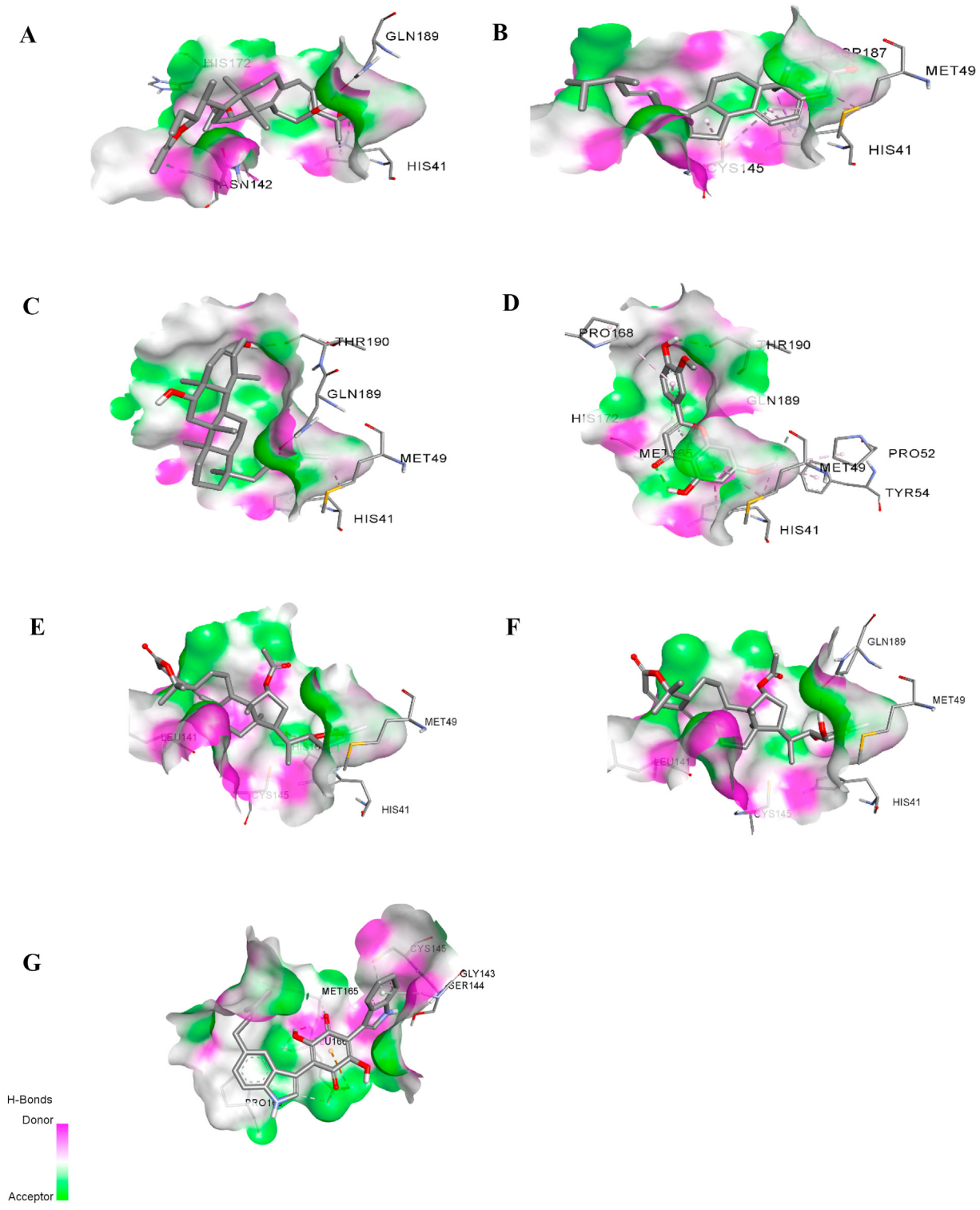

Fig. 3. Hydrogen bond interactions between 6LU7 and (A) colossolactone G, (B) ergosterol, (C) heliantriol F, (D) velutin, (E) colossolactone VIII, (F) colossolactone E and (G) semicochliodinol A.

HIV protease and anti-inflammatory activities. Those compounds may have the potential to inhibit SARS-CoV-2 main protease and become useful for the treatment of COVID-19 patients. In this study, mushroom-derived compounds were docked against the main viral protease. In addition, the *in silico* ADME analysis and toxicity of these compounds were conducted to predict their drug-like properties, toxicity, carcinogenicity and mutagenicity. Our study revealed six compounds found in mushrooms, namely colossolactone VIII, colossolactone E colossolactone G, ergosterol, heliantriol F and velutin the best potential candidates for anti-SAR-CoV-2 agents. Those potential compounds could be used and developed as an alternative or complementary medicine for COVID-19 treatment. Moreover, ergosterol has been reported as an anti-inflammatory agent.[86,87] These could support the idea of ergosterol being a

useful compound for COVID-19 treatment due to its dual activities. Strategies are in place to confirm theirs *in vitro* inhibitory activity against SARS-CoV-2 protease and toxicity in healthy mammalian cells such as human PBMCs. The discovery of such inhibitors with low or no toxicity would provide us with further opportunity to develop them into anti-COVID-19 in monotherapy or combination drugs.

Declaration of competing interest

The authors declare that they have no known competing financial interests or personal relationships that could have appeared to influence the work reported in this paper.

Acknowledgements

This research project is supported by the Second Century Fund (C2F), Chulalongkorn University, Bangkok, Thailand for Panthakarn Rangsinth's postdoctoral fellowship.

Appendix A. Supplementary data

Supplementary data to this article can be found online at https://doi.org/10.1016/j.jtcme.2020.12.002.

References

1. World Health Organization. *Coronavirus disease (COVID-19) Situation Report*. World Health Organization; 27 December 2020.
2. Chen N, Zhou M, Dong X, et al. Epidemiological and clinical characteristics of 99 cases of 2019 novel coronavirus pneumonia in Wuhan, China: a descriptive study. *Lancet (London, England)*. 2020;395(10223):507–513.
3. Wang D, Hu B, Hu C, et al. Clinical characteristics of 138 hospitalized patients with 2019 novel coronavirus-infected pneumonia in wuhan, China. *Jama*. 2020;323(11):1061–1069.
4. Zhu N, Zhang D, Wang W, et al. A novel coronavirus from patients with pneumonia in China, 2019. *N Engl J Med*. 2020;382(8):727–733.
5. Cui J, Li F, Shi ZL. Origin and evolution of pathogenic coronaviruses. *Nat Rev Microbiol*. 2019;17(3):181–192.
6. Jin Z, Du X, Xu Y, et al. Structure of M(pro) from COVID-19 virus and discovery of its inhibitors. *Nature*. 2020;582:289–293.
7. Jin Z, Zhao Y, Sun Y, et al. Structural basis for the inhibition of SARS-CoV-2 main protease by antineoplastic drug carmofur. *Nat Struct Mol Biol*. 2020;27:529–532.
8. Dai W, Zhang B, Su H, et al. *Structure-based design of antiviral drug candidates targeting the SARS-CoV-2 main protease*. 6497th 368. New York, NY: Science; 2020:1331–1335.
9. Pillaiyar T, Manickam M, Namasivayam V, Hayashi Y. Jung S-HJJomc. An overview of severe acute respiratory syndrome–coronavirus (SARS-CoV) 3CL protease inhibitors. *Peptidomimetics Small Mol. Chemother*. 2016;59(14):6595–6628.
10. Kumar V, Shin JS, Shie JJ, et al. Identification and evaluation of potent Middle East respiratory syndrome coronavirus (MERS-CoV) 3CL(Pro) inhibitors. *Antivir Res*. 2017;141:101–106.
11. Kumar V, Tan KP, Wang YM, Lin SW, Liang PH. Identification, synthesis and evaluation of SARS-CoV and MERS-CoV 3C-like protease inhibitors. *Bioorg Med Chem*. 2016;24(13):3035–3042.
12. Anand K, Ziebuhr J, Wadhwani P, Mesters JR, Hilgenfeld R. Coronavirus main proteinase (3CLpro) structure: basis for design of anti-SARS drugs. *Science*. 2003;300(5626):1763–1767.
13. Yang H, Xie W, Xue X, et al. Design of wide-spectrum inhibitors targeting coronavirus main proteases. *PLoS Biol*. 2005;3(10). e324.
14. Tsuji M. Potential anti-SARS-CoV-2 drug candidates identified through virtual screening of the ChEMBL database for compounds that target the main coronavirus protease. *FEBS open bio*. 2020;10(6):995–1004.
15. Serafin MB, Bottega A, Foletto VS, da Rosa TF, Hörner A, Hörner R. Drug repositioning is an alternative for the treatment of coronavirus COVID-19. *Int J Antimicrob Agents*. 2020:105969.
16. Tu YF, Chien CS, Yarmishyn AA, et al. A review of SARS-CoV-2 and the ongoing clinical trials. *Int J Mol Sci*. 2020;21(7).
17. Chu CM, Cheng VC, Hung IF, et al. Role of lopinavir/ritonavir in the treatment of SARS: initial virological and clinical findings. *Thorax*. 2004;59(3):252–256.
18. Arabi YM, Alothman A, Balkhy HH, et al. Treatment of Middle East Respiratory Syndrome with a combination of lopinavir-ritonavir and interferon-β1b (MIRACLE trial): study protocol for a randomized controlled trial. *Trials*. 2018;19(1):81.
19. Zumla A, Chan JF, Azhar EI, Hui DS, Yuen KY. Coronaviruses - drug discovery and therapeutic options. *Nat Rev Drug Discov*. 2016;15(5):327–347.
20. Nutho B, Mahalapbutr P, Hengphasatporn K, et al. Why are lopinavir and ritonavir effective against the newly emerged coronavirus 2019? Atomistic insights into the inhibitory mechanisms. *Biochemistry*. 2020;59(18):1769–1779.
21. Sheahan TP, Sims AC, Leist SR, et al. Comparative therapeutic efficacy of remdesivir and combination lopinavir, ritonavir, and interferon beta against MERS-CoV. *Nat Commun*. 2020;11(1):222.
22. Kim JY, Choe PG, Oh Y, et al. The first case of 2019 novel coronavirus pneumonia imported into Korea from Wuhan, China: implication for infection prevention and control measures. *J Kor Med Sci*. 2020;35(5). e61.
23. Qiu H, Wu J, Hong L, Luo Y, Song Q, Chen D. Clinical and epidemiological features of 36 children with coronavirus disease 2019 (COVID-19) in Zhejiang, China: an observational cohort study. *The Lancet Infectious disea*. 2020;20(6):689–696.
24. Ye XT, Luo YL, Xia SC, et al. Clinical efficacy of lopinavir/ritonavir in the treatment of Coronavirus disease 2019. *Eur Rev Med Pharmacol Sci*. 2020;24(6):3390–3396.
25. Cao B, Wang Y, Wen D, et al. A trial of lopinavir-ritonavirses in adults hospitalized with severe COVID-19. *N Engl J Med*. 2020;382(19):1787–1799.
26. Fuzimoto AD, Isidoro C. The antiviral and coronavirus-host protein pathways inhibiting properties of herbs and natural compounds - additional weapons in the fight against the COVID-19 pandemic? *J Tradit, Complementary Med*. 2020;10(4):405–419.
27. Benarba B, Pandiella A. *Medicinal plants as sources of active molecules against COVID-19*11. Front Pharmacol.; 2020:1–16.
28. Bhuiyan FR, Howlader S, Raihan T, Hasan M. *Plants metabolites: possibility of natural therapeutics against the COVID-19 pandemic*7. Front Med (Lausanne); 2020:1–26.
29. Prasansuklab A, Theerasri A, Rangsinth P, Sillapachaiyaporn C, Chuchawankul S, Tencomnao T. Anti-COVID-19 drug candidates: a review on potential biological activities of natural products in the management of new coronavirus infection. *J Tradit Complement Med*; 2020. https://doi.org/10.1016/j.jtcme.2020.12.001. In press.
30. Singh R, Bhardwaj V, Das P, Purohit R. Natural analogues inhibiting selective cyclin-dependent kinase protein isoforms: a computational perspective. *J Biomol Struct Dynam*. 2020;38(17):5126–5135.
31. Bhardwaj V, Singh R, Singh P, Purohit R, Kumar S. Elimination of bitter-off taste of stevioside through structure modification and computational interventions. *J Theor Biol*. 2020;486:110094.
32. Bhardwaj VK, Purohit R. Targeting the protein-protein interface pocket of Aurora-A-TPX2 complex: rational drug design and validation. *J Biomol Struct Dyn*. 2020:1–10.
33. Sharma J, Bhardwaj VK, Das P, Purohit R. Identification of naturally originated molecules as γ-aminobutyric acid receptor antagonist. *J Biomol Struct Dyn*. 2020:1–12.
34. Bhardwaj VK, Singh R, Sharma J, Das P, Purohit R. Structural based study to identify new potential inhibitors for dual specificity tyrosine-phosphorylation-regulated kinase. *Comput Methods Progr Biomed*. 2020;194:105494.
35. Bhardwaj VK, Singh R, Sharma J, Rajendran V, Purohit R, Kumar S. Identification of bioactive molecules from tea plant as SARS-CoV-2 main protease inhibitors. *J Biomol Struct Dyn*. 2020:1–10.
36. Enmozhi SK, Raja K, Sebastine I, Joseph J. Andrographolide as a potential inhibitor of SARS-CoV-2 main protease: an *in silico* approach. *J Biomol Struct Dynam*. 2020:1–7.
37. Kumar A, Choudhir G, Shukla SK, et al. Identification of phytochemical inhibitors against main protease of COVID-19 using molecular modeling approaches. *J Biomol Struct Dyn*. 2020:1–11.
38. Gogoi N, Chowdhury P, Goswami AK, Das A, Chetia D, Gogoi B. Computational guided identification of a citrus flavonoid as potential inhibitor of SARS-CoV-2 main protease. *Mol Divers*. 2020:1–15.
39. Uniyal A, Mahapatra MK, Tiwari V, Sandhir R, Kumar R. Targeting SARS-CoV-2 main protease: structure based virtual screening, *in silico* ADMET studies and molecular dynamics simulation for identification of potential inhibitors. *J Biomol Struct Dynam*. 2020:1–17.
40. Rajagopal K, Varakumar P, Baliwada A, Byran G. Activity of phytochemical constituents of *Curcuma longa* (turmeric) and *Andrographis paniculata* against coronavirus (COVID-19): an *in silico* approach. *Future J Pharmaceut Sci*. 2020;6(1):104.
41. Linnakoski R, Reshamwala D, Veteli P, Cortina-Escribano M, Vanhanen H, Marjomäki V. Antiviral agents from fungi: diversity, mechanisms and potential applications. *Front Microbiol*. 2018;9:2325.
42. Suwannarach N, Kumla J, Sujarit K, Pattananandecha T, Saenjum C, Lumyong S. Natural bioactive compounds from fungi as potential candidates for protease inhibitors and immunomodulators to apply for coronaviruses. *Molecules (Basel, Switzerland)*. 2020;25(8).
43. Elsayed EA, El Enshasy H, Wadaan MA, Aziz R. Mushrooms: a potential natural source of anti-inflammatory compounds for medical applications. *Mediat Inflamm*. 2014;2014:805841.
44. Muszyńska B, Grzywacz-Kisielewska A, Kała K, Gdula-Argasińska J. Anti-inflammatory properties of edible mushrooms: a review. *Food Chem*. 2018;243:373–381.
45. Nallathamby N, Phan CW, Seow SL, et al. A status review of the bioactive activities of tiger milk mushroom *Lignosus rhinocerotis* (cooke) Ryvarden. *Front Pharmacol*. 2017;8:998.

46. Sato N, Zhang Q, Ma C-M, Hattori M. Anti-human immunodeficiency virus-1 protease activity of new lanostane-type triterpenoids from *Ganoderma sinense*. *Chem Pharm Bull*. 2009;57(10):1076–1080.
47. Ngai PH, Zhao Z, Ng TB. Agrocybin, an antifungal peptide from the edible mushroom *Agrocybe cylindracea*. *Peptides*. 2005;26(2):191–196.
48. Kashiwada Y, Hashimoto F, Cosentino LM, Chen CH, Garrett PE, Lee KH. Betulinic acid and dihydrobetulinic acid derivatives as potent anti-HIV agents. *J Med Chem*. 1996;39(5):1016–1017.
49. Habibi E, Sadat-Ebrahimi SE, Mousazadeh SA, Amanzadeh Y. Mycochemical investigation of the Turkey tail medicinal mushroom *Trametes versicolor* (higher basidiomycetes): a potential application of the isolated compounds in documented pharmacological studies. *Int J Med Mushrooms*. 2015;17(3):255–265.
50. El Dine RS, El Halawany AM, Ma C-M, Hattori M. Anti-HIV-1 protease activity of lanostane triterpenes from the Vietnamese mushroom *Ganoderma colossum*. *J Nat Prod*. 2008;71(6):1022–1026.
51. Modi M, Goel T, Das T, et al. Ellagic acid & gallic acid from *Lagerstroemia speciosa* L. inhibit HIV-1 infection through inhibition of HIV-1 protease & reverse transcriptase activity. *Indian J Med Res*. 2013;137(3):540–548.
52. Hu Q, Yuan B, Xiao H, et al. Polyphenols-rich extract from *Pleurotus eryngii* with growth inhibitory of HCT116 colon cancer cells and anti-inflammatory function in RAW264.7 cells. *Food & function*. 2018;9(3):1601–1611.
53. Rahman MA, Abdullah N, Aminudin N. Antioxidative effects and inhibition of human low density lipoprotein oxidation in vitro of polyphenolic compounds in *Flammulina velutipes* (golden needle mushroom). *Oxidative Medicine and Cellular Longevity*. 2015;2015:1–10.
54. Lee YS, Kang YH, Jung JY, et al. Inhibitory constituents of aldose reductase in the fruiting body of *Phellinus linteus*. *Biol Pharm Bull*. 2008;31(4):765–768.
55. Sillapachaiyaporn C, Nilkhet S, Ung AT, Chuchawankul S. Anti-HIV-1 protease activity of the crude extracts and isolated compounds from *Auricularia polytricha*. *BMC Compl Alternative Med*. 2019;19(1):351.
56. Tong S, Zhong H, Yi C, et al. Simultaneous HPLC determination of ergosterol and 22,23-dihydroergosterol in *Flammulina velutipes* sterol-loaded microemulsion. *Biomed Chromatogr : BMC (Biomed Chromatogr)*. 2014;28(2):247–254.
57. Rahman MA, Abdullah N, Aminudin N. *Lentinula edodes* (shiitake mushroom): an assessment of *in vitro* anti-atherosclerotic bio-functionality. *Saudi J Biol Sci*. 2018;25(8):1515–1523.
58. Sevindik M, Rasul A, Hussain G, et al. Determination of anti-oxidative, antimicrobial activity and heavy metal contents of *Leucoagaricus leucothites*. *Pak J Pharm Sci*. 2018;31(5):2163–2168.
59. Gaur T, Rao PB. Analysis of antibacterial activity and bioactive compounds of the giant mushroom, *Macrocybe gigantea* (agaricomycetes), from India. *Int J Med Mushrooms*. 2017;19(12):1083–1092.
60. Liu J, Jia L, Kan J, Jin CH. *In vitro* and *in vivo* antioxidant activity of ethanolic extract of white button mushroom (*Agaricus bisporus*). *Food Chem Toxicol : Int J Publ Br Ind Biol Res Assoc*. 2013;51:310–316.
61. Yoon KN, Alam N, Lee KR, et al. Antioxidant and antityrosinase activities of various extracts from the fruiting bodies of *Lentinus lepideus*. *Molecules (Basel, Switzerland)*. 2011;16(3):2334–2347.
62. Karaman M, Jovin E, Malbasa R, Matavuly M, Popović M. Medicinal and edible lignicolous fungi as natural sources of antioxidative and antibacterial agents. *Phytother Res : PTR*. 2010;24(10):1473–1481.
63. el-Mekkawy S, Meselhy MR, Nakamura N, et al. Anti-HIV-1 and anti-HIV-1-protease substances from *Ganoderma lucidum*. *Phytochemistry*. 1998;49(6):1651–1657.
64. Akbar R, Yam WK. Interaction of ganoderic acid on HIV related target: molecular docking studies. *Bioinformation*. 2011;7(8):413–417.
65. Min BS, Nakamura N, Miyashiro H, Bae KW, Hattori M. Triterpenes from the spores of *Ganoderma lucidum* and their inhibitory activity against HIV-1 protease. *Chem Pharm Bull (Tokyo)*. 1998;46(10):1607–1612.
66. El Dine RS, El Halawany AM, Ma C-M, Hattori M. Inhibition of the dimerization and active site of HIV-1 protease by secondary metabolites from the Vietnamese mushroom *Ganoderma colossum*. *J Nat Prod*. 2009;72(11):2019–2023.
67. Sillapachaiyaporn C, Chuchawankul S. HIV-1 protease and reverse transcriptase inhibition by tiger milk mushroom (*Lignosus rhinocerus*) sclerotium extracts: *in vitro* and *in silico* studies. *J Tradit Complement Med*. 2019;10(4):396–404.
68. Wang CR, Zhou R, Ng TB, Wong JH, Qiao WT, Liu F. First report on isolation of methyl gallate with antioxidant, anti-HIV-1 and HIV-1 enzyme inhibitory activities from a mushroom (*Pholiota adiposa*). *Environ Toxicol Pharmacol*. 2014;37(2):626–637.
69. Mengoni F, Lichtner M, Battinelli L, et al. In vitro anti-HIV activity of oleanolic acid on infected human mononuclear cells. *Planta Med*. 2002;68(2):111–114.
70. Zhang CC, Yin X, Cao CY, Wei J, Zhang Q, Gao JM. Chemical constituents from *Hericium erinaceus* and their ability to stimulate NGF-mediated neurite outgrowth on PC12 cells. *Bioorg Med Chem Lett*. 2015;25(22):5078–5082.
71. Kalogeropoulos N, Yanni AE, Koutrotsios G, Aloupi M. Bioactive microconstituents and antioxidant properties of wild edible mushrooms from the island of Lesvos, Greece. *Food Chem Toxicol : Int J Publ Br Ind Biol Res Assoc*. 2013;55:378–385.
72. Fredenhagen A, Petersen F, Tintelnot-Blomley M, Rösel J, Mett H, Hug P. Semicochliodinol A and B: inhibitors of HIV-1 protease and EGF-R protein tyrosine kinase related to asterriquinones produced by the fungus *Chrysosporium merdarium*. *J Antibiot*. 1997;50(5):395–401.
73. Ma C, Nakamura N, Miyashiro H, Hattori M, Shimotohno K. Inhibitory effects of constituents from *Cynomorium songaricum* and related triterpene derivatives on HIV-1 protease. *Chem Pharm Bull (Tokyo)*. 1999;47(2):141–145.
74. Wang H, Ng TB. Isolation and characterization of velutin, a novel low-molecular-weight ribosome-inactivating protein from winter mushroom (*Flammulina velutipes*) fruiting bodies. *Life Sci*. 2001;68(18):2151–2158.
75. Daina A, Michielin O, Zoete V. SwissADME: a free web tool to evaluate pharmacokinetics, drug-likeness and medicinal chemistry friendliness of small molecules. *Sci Rep*. 2017;7:42717.
76. Pires DEV, Blundell TL, Ascher DB. pkCSM: predicting small-molecule pharmacokinetic and toxicity properties using graph-based signatures. *J Med Chem*. 2015;58(9):4066–4072.
77. Benigni R, Bossa C, Jeliazkova N, Netzeva T, Worth A. *The Benigni/Bossa rulebase for mutagenicity and carcinogenicity – a module of Toxtree*. OPOCE; 2008:1–78.
78. Benigni R, Bossa C, Netzeva T, Rodomonte A, Tsakovska I. Mechanistic QSAR of aromatic amines: new models for discriminating between homocyclic mutagens and nonmutagens, and validation of models for carcinogens. *Environ Mol Mutagen*. 2007;48(9):754–771.
79. Gibbs JW. *A Method of Geometrical Representation of the Thermodynamic Properties by Means of Surfaces*. *Transactions of the Connecticut Academy of Arts and Sciences*2. New Haven; 1873:382–404.
80. Khaerunnisa S, Kurniawan H, Awaluddin R, Suhartati S, Soetjipto S. *Potential inhibitor of COVID-19 main protease (Mpro) from several medicinal plant compounds by molecular docking study*1. Preprints; 2020:1–14.
81. Islam R, Parves MR, Paul AS, et al. A molecular modeling approach to identify effective antiviral phytochemicals against the main protease of SARS-CoV-2. *J Biomol Struct Dynam*. 2020:1–12.
82. Gyebi GA, Ogunro OB, Adegunloye AP, Ogunyemi OM, Afolabi SO. Potential inhibitors of coronavirus 3-chymotrypsin-like protease (3CL(pro)): an *in silico* screening of alkaloids and terpenoids from African medicinal plants. *J Biomol Struct Dynam*. 2020:1–13.
83. Kumar A, Choudhir G, Shukla SK, et al. Identification of phytochemical inhibitors against main protease of COVID-19 using molecular modeling approaches. *J Biomol Struct Dynam*. 2020:1–21.
84. Lipinski CA, Lombardo F, Dominy BW, Feeney PJ. Experimental and computational approaches to estimate solubility and permeability in drug discovery and development settings. *Adv Drug Deliv Rev*. 2001;46(1-3):3–26.
85. Nasution MAF, Toepak EP, Alkaff AH, Tambunan USF. Flexible docking-based molecular dynamics simulation of natural product compounds and Ebola virus Nucleocapsid (EBOV NP): a computational approach to discover new drug for combating Ebola. *BMC Bioinf*. 2018;19(Suppl 14):419.
86. Liu C, Zhao S, Zhu C, et al. Ergosterol ameliorates renal inflammatory responses in mice model of diabetic nephropathy. *Biomedicine & pharmacotherapy*. 2020;128:110252.
87. Sun X, Feng X, Zheng D, et al. Ergosterol attenuates cigarette smoke extract-induced COPD by modulating inflammation, oxidative stress and apoptosis *in vitro* and *in vivo*. *Clinical science (London, England: 1979)*. 2019;133(13):1523–1536.